

Full Research Paper

Rotational Spectra of Symmetric Top Molecules in Ground and Different Vibrational Excited States, and Phenomenon of Resonance – Applying in CF₃CCH

Masoud Motamedi*

Department of Chemistry, Faculty of Science, University of Kurdistan, Sanandaj, Iran;

E-mail: motamedimas@yahoo.co.uk

* Author to whom correspondence should be addressed.

Received: 13 February 2007 / Revised version accepted: 23 March 2007 / Published: 17 April 2007

Abstract: This paper deals with review of exploration of resonance in symmetric top molecules in different vibrational excited states, $v_t = n$ ($n = 1, 2, 3, 4$). Calculations for CF₃CCH shows that resonance take place at $k = \frac{x_{\ell\ell} + (A - B) - 2A\zeta}{A\zeta - (A - B)}$ and

$k = \frac{x_{\ell\ell} + (A - B) - 2A\zeta}{A\zeta - (A - B)}$ for $v_{10} = 2$ and $v_{10} = 3$ respectively. In order to account for splitting

about 3 MHz for the - 2 series in $v_{10} = 4$ is necessary to introduce the element $\langle J, k, \ell | f_{24} | J, k + 2, \ell - 4 \rangle$ in fitting program.

Keywords: excited states, resonance, CF₃CCH, symmetric top molecules

1. Introduction

The vibrational spectrum of CF₃CCH was assigned by Berney et al [1]. The energy level of its lowest lying degenerate vibration is only $E = 171 \text{ cm}^{-1}$, consequently according to the Boltzman distribution law it has a population of 58% ($29\% \times 2$ for vibrational degeneracy) of the ground state at dry ice temperature (200 K). Therefore the rotational spectrum in the $v_{10} = 1$ state is also strong and it is not complicated by interactions with nearby vibrational states. Whereas it is a prolate top, its rotational constants $A \approx 5.7$ and $B \approx 2.9$ GHz are not large. So, it is a possible candidate for the

observation of the A_1 - A_2 splitting in the ground state. The q_1^+ is rather large and $A - B - A\zeta$ is small and it is possible to observe direct ℓ -type resonance transitions in the microwave range [2]. These situation have been previously observed only for PF_3 , $v_4 = 1$ [3], for CF_3H and CF_3D , $v_6 = 1$ [4], CF_3Cl , $v_6 = 1$ [5] and CH_3CF_3 , $v_{12} = 1$ [6]. The rotational spectra of CF_3CCD , the isotopomer of this molecule in the ground, $v_{10} = 1$ and $v_{10} = 2$ states have been measured and studied by several authors [7-11].

Three identical fluorine atoms ($I = 1/2$) in CF_3CCH have important consequences in the determination of relative intensities of signals. The symmetry operations like exchange of nuclei, have symmetric effect on the total wavefunction for nuclei with integral or zero spin (Bose particles). But for nuclei with half integral spin (Fermi particles) the total wavefunction is antisymmetric. The rotation about the C_3 axis through $2\pi/3$ or $4\pi/3$ rotation is equal to two exchanges of nuclei. Therefore it is symmetric (A) for Fermi particles as well as Bose particles. A rotation of $2\pi/3$ about top axis will not change ψ_{rot} states with $k = 3n$ ($n = \text{integer}$, including $n = 0$) since $\psi_{\text{rot}} \propto e^{ik\psi}$. For the symmetric state, the species are A and in antisymmetric state ($k \neq 3n$) the species are E. There are eight different possibilities for combinations of three fluorine atoms with spin $1/2$. Two of them can occur when three spins are the same $1/2$ or $-1/2$, these are totally symmetric because they remain unchanged by any permutation of nuclei which are equivalent to a rotation. But this situation can not take place for the remaining 6 arrangements, which are $2A_1 + 2E$. So the 8 spin functions are $4A_1 + 2E$. The statistical weight depends on the ratio between the spin function of symmetry A and the spin function of symmetry E. Consequently:

The intensity of A rotational states = 2 (intensity of E rotational states)

For symmetric top molecules like CF_3CCH , the ground vibrational state rotational energies are given up to sextic terms by equation (1) and by application of selection rules $\Delta J = +1$ and $\Delta k = 0$, the frequencies are given by equation (2).

$$E_{J,k} = BJ(J+1) + (A-B)k^2 - D_J J^2(J+1)^2 - D_{JK} J(J+1)k^2 - D_k k^4 + H_J J^3(J+1)^3 + H_{JK} J^2(J+1)^2 k^2 + H_{kJ} J(J+1)k^4 + H_k k^6 \quad (1)$$

$$\nu = 2B(J+1) - 4D_J(J+1)^3 - 2D_{JK}(J+1)k^2 + H_J(J+1)^3[(J+2)^3 - J^3] + 4H_{JK}(J+1)^3 k^2 + 2H_{kJ}(J+1)k^4 \quad (2)$$

The spectra in this state are simple, so the different k values ($k = 0, 1, 2, 3, 4, \dots$) for each J transition are assigned easily. This is illustrated in Figure 1, which shows part of the observed transition $J = 24 \rightarrow 25$, and compares it with the calculated spectrum.

The centrifugal distortion produces a band head to high frequency at $k = 0$, with a spread to lower frequency with higher k Figure 2. Due to negative value of D_{JK} for CH_3Cl , this situation is different Figure 3.

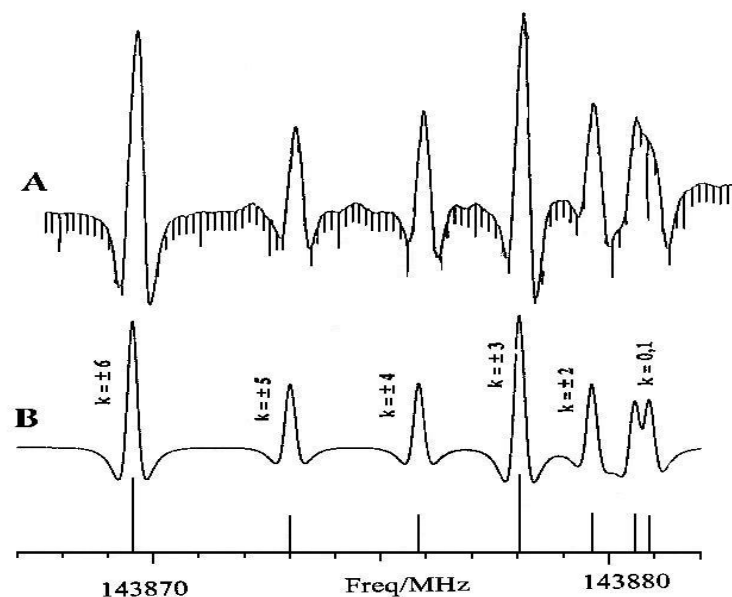


Figure 1. Part of the $J = 24 \rightarrow 25$ spectrum of CF_3CCH in ground state. The top trace (A) is the observed spectrum, the lower (B) is a computer simulation.

If $|k|$ values are plotted against frequency for this state, the Fortrat diagrams are produced which are shown in Figures 2,3. In these diagrams the splitting increase as k increases and this is due to the D_{Jk} parameter. D_{Jk} is 6.27 and -2.517 kHz for CF_3CCH and CHCl_3 respectively [2, 12].

The sextic centrifugal distortion constants were accurately determined for the first time for the ground state, and result shows that $H_{Jk} > |H_{kJ}|$ and $H_{kJ} < 0$. For this molecule the sextic splitting constant h_3 is very small [2]. Cazzoli et al. [13] have found amount of this value, which is $h_3 = 2.3 \times 10^{-21} \frac{B^4}{A-B}$. The predicted value of h_3 for CF_3CCH , 2.6×10^{-11} MHz, gives a splitting about 12 MHz for the highest - J transition ($J = 112$) [2].

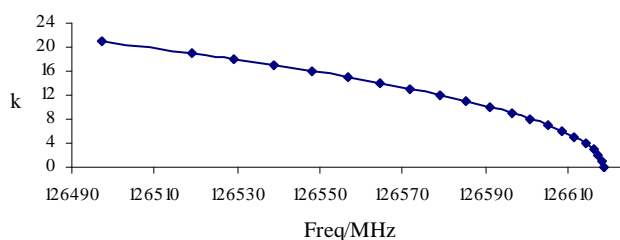


Figure 2. Fortrat diagram of CF_3CCH in ground state $J = 21 \rightarrow 22$.

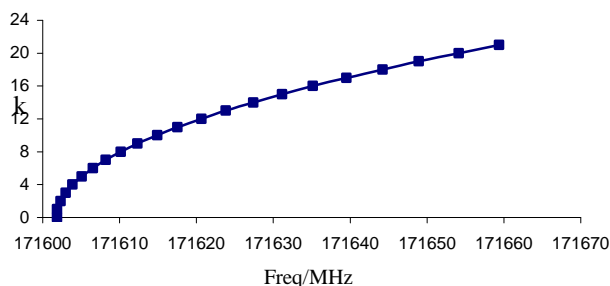


Figure 3. Fortrat diagram of CHCl_3 in ground state $J = 21 \rightarrow 22$.

2. Rotation Spectrum in Excited State $\nu_{10} = 1$

Because ν_{10} state of this molecule has a high population, the rotational spectra in this state are also strong. It is isolated in frequency from other vibrational states, so is not complicated by interactions with nearby states.

Rotational frequencies for transitions $J \rightarrow J + 1$ in the excited degenerate vibrational state $\nu_t = 1$, $\ell_t = \pm 1$ of molecules with axial symmetry were calculated by Nielsen [14]. Although the Nielsen theory was fairly satisfactory for the rotation spectrum of these type of molecules, some of the calculated frequencies by this method were different from the observed frequencies. This formula was extended to the case of higher J value by Gordy et al. [7]. They also interpreted the transitions $J = 4 \rightarrow 5$ and $J = 8 \rightarrow 9$ of CF_3CCH in the excited state $\nu_{10} = 1$. Then the frequencies of lines for transition $J \rightarrow J + 1$ were investigated and calculated for $\nu_t = 1$ and $\nu_t = 2$ states [15, 16].

The frequency of transition $J \rightarrow J + 1$ for molecules belonging to the point group C_{3v} in singly excited vibrational state $\nu_t = 1$, is given by the approximate perturbation expression, equation (3).

$$\nu = 2B(J + 1) - 4D_J(J + 1)^3 - 2D_{Jk}(J + 1)k^2 + 2\eta_J(J + 1)k\ell + \Delta\nu \quad (3)$$

where $\Delta\nu$ has the value $\pm q_t^+(J + 1)$ if $(k\ell - 1) = 0$ (ℓ -type doubling) or

$$\Delta\nu = -\frac{(q_t^+)^2(J + 1)^3}{4(B - A + A\zeta)(k\ell - 1)} \quad \text{if } (k\ell - 1) \neq 0 \quad (\ell\text{-type resonance}) \quad (4)$$

Where ζ is the ℓ -type doubling constant, B and A are rotational constants, and ζ is the z-coriolis constant for the vibrational state ν_t . The degree of ℓ -resonance thus largely depends on the ratio of q_t^+ to the resonance denominator $(B - A + A\zeta)$. With low to moderate values of this denominator, the spectrum usually found consists of two extreme outer lines for $(k\ell - 1) = 0$ (the ℓ -doublets) and a center group of lines for $(k\ell - 1) \neq 0$ whose structure depends very strongly on other parameters such as the centrifugal distortion constants. As the strength of the resonance increase, the lines of the center group

spread out until the low $|k\ell-1|$ transitions approach the positions of the ℓ -doublets. So for large q_t^+ and small ($A - B - A\zeta = -458$ MHz) value it is possible to observe direct ℓ -resonance transitions in the microwave range. This is a typical pattern for C_{3v} doubly degenerate states and is predominantly due to the combinations of the splitting of the positive and negative $(k\ell-1)$ series by ℓ -type resonance [which is inversely proportional to $(k\ell-1)$] and the shift to low frequency due to D_{JK} [which is proportional to $(k\ell-1)^2$]. Thus one series goes from high frequency at low k to low frequency at high k , while the other is at low frequency both for high and low k , with a head at some intermediate value.

In order to obtain more accuracy than can be obtained from perturbation theory in rotational energies for singly excited vibrational states it is necessary to set up the rotational Hamiltonian as a matrix (H) in equation $H\psi = E\psi$ and diagonalise to obtain the energy (2,10,11,17,18,21,22). This is particularly necessary when $[B - A + (A\zeta)]$ is small in the above equation; the diagonalization avoids the errors implicit in perturbation theory or the need to go to higher orders of perturbation.

The Hamiltonian is set up for a symmetric top molecule like CF_3CCH [2, 11]. This rotation-vibrational Hamiltonian has two different blocks belong to the different $\ell = +1$ and $\ell = -1$ series. k and ℓ are no longer good quantum numbers but $(k - \ell)$ or $(k\ell - 1)$ may be used to distinguish between the symmetry species; those levels with $(k\ell - 1) = 3n$, where n is an integer, are of species A_1 or A_2 . If $(k\ell - 1) \neq 3n$ the species are E . The q_t^+ produces a first order splitting of the $(k\ell - 1) = 0$, A_1A_2 pair which are the familiar ℓ -doublets, as shown by Grenier-Besson and Amat and others [2, 10, 11, 15, 19]. The main difference from the ground state spectra is the splitting of the $|k - \ell| = 0$ into two widely separate ℓ -doublets and the splitting, due to ℓ -resonance. Where ℓ is the vibration angular momentum quantum number and ζ is the Coriolis coupling coefficient. Hence k and ℓ are not good quantum numbers, though $k\ell - 1$ may be used as a satisfactory label.

The diagonal elements of the Hamiltonian used were:

$$\begin{aligned} \langle v_t, \ell_t, J, k | H/h | v_t, \ell_t, J, k \rangle = & BJ(J+1) + (A-B)k^2 - 2A\zeta k\ell - D_J J^2(J+1)^2 \\ & - D_{JK} J(J+1)k^2 - D_k k^4 + H_J J^3(J+1)^3 + H_{JK} J^2(J+1)^2 k^2 + H_{kJ} J(J+1)k^4 + H_k k^6 \\ & + \eta_J J(J+1)k\ell + \eta_k k^3\ell \end{aligned} \quad (5)$$

In addition there are off-diagonal elements given by:

$$\begin{aligned} \langle v_t, \ell, J, k | H/h | v_t, \ell \pm 2, J, k \pm 2 \rangle \\ = -\frac{1}{4} q_t^+ \{ (v_t \mp \ell)(v_t \pm \ell + 2)[J(J+1) - k(k \pm 1)] \times [J(J+1) - (k \pm 1)(k \pm 2)] \}^{1/2} \end{aligned} \quad (6)$$

and $\langle v_t, \ell, J, k | H/h | v_t, \ell \pm 2, J, k \mp 1 \rangle$

$$= r_t [(v_t+1)^2 - (\ell \pm 1)^2]^{1/2} [J(J+1) - k(k \mp 1)]^{1/2} (2k \mp 1).$$

In equation 5, the D_J , D_{JK} , D_K are quartic, H_J , H_{JK} , H_{KJ} are sextic centrifugal distortion terms respectively. ζ is the Coriolis coupling coefficient between the two components of the degenerate state and η_J represents the centrifugal distortion of $(A\zeta)$. The general effect of the additional parameters to complicate the spectrum relative to that of a non-degenerate state.

If $|k\ell - 1|$ values are plotted against frequency for this state, the Fortrat-diagram is produced which is shown for CH_3CCH in Figure 4. This diagram shows the ' ℓ ' doublet and two different series $\ell = \pm 1$. So the spectrum is more complex compared with ground state [2].

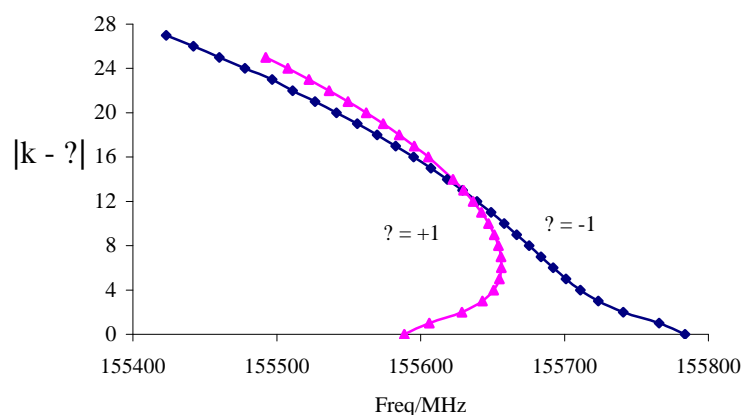


Figure 4. Fortrat diagram of CF_3CCH in $\nu_{10} = 1$ state. $J = 20 \rightarrow 21$.

In the present example the rotational Hamiltonian was diagonalised to give exact ℓ -resonance shifts. The spectrum in the millimetre-wave should consist of two widely spaced lines, the ℓ -doublets, whose separation is given by equation (4), and a central group of transitions with $|k\ell - 1| > 0$, whose frequencies are determined by equation (3). In the latter set the transitions with low values of $|k\ell - 1|$ will tend to lie towards the outsides of the group since their ℓ -resonance shifts as predicted by equation (3) will be large. Two series should thus be observed depending on the sign of $k\ell - 1$. There are two different series in spectrum, making it more difficult to assign than the ground state Figure 4.

3. Rotational Spectra in Excited States, $\nu_{10} = 2, 3, 4$

The vibrational level $\nu_{10} = 2$ is located at 342 cm^{-1} . The vibrational levels closest to $\nu_{10} = 2$ are $\nu_5 = 1$ and $\nu_9 = 1$ at 536 and 452 cm^{-1} , respectively [2, 9, 20-22]. As the analysis will show, the level can be considered as being isolated and an effective Hamiltonian for a $\nu_t = 2$ level is suitable for the analysis of the data. The general features of the direct ℓ -resonance transitions in the $\nu_t = 2$ level have been discussed by Harder et al. [21]. There is a good agreement for the obtained rotational constants B and the ℓ -dependence $\gamma_{\ell\ell} = (B_2 - B_0)/4$. Because the main information is obtained from the data of Carpenter et al [20]. The fact that the direct ℓ -type resonance transitions provide further information on [21]. Excellent agreement is obtained for the values of $g_{\ell\ell} = E_v^2 - E_v^0/4$, because the parameter A constrained in its value [20]. The B and other spectroscopic constants determined accurately up to $\nu_{10} = 4$ and show a regular dependence on the vibrational quantum number Figure 5 [2, 20, 22, 23].

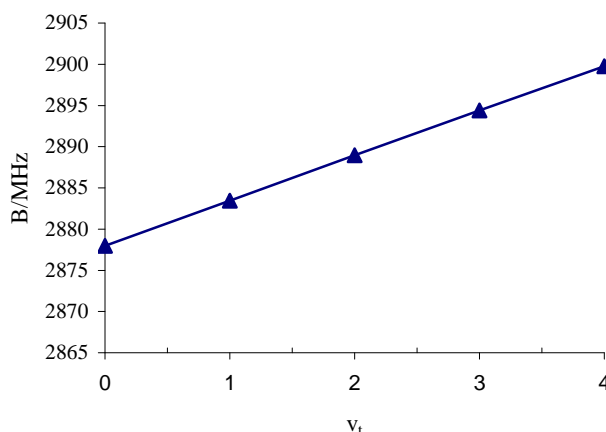


Figure 5. Plot of B against v_t for CF₃CCH.

These spectra show no obvious regularity from the point of view of frequencies as well as intensities, because there are three series for each J since the vibrational angular momentum quantum number ℓ can have values 0 and ± 2 . Therefore it is difficult to identify the quantum numbers k and ℓ associated with each absorption in these spectra. However from the point of view of experimental work, correspondence between the lines of different J value should be observed with respect to their relative position as well as their intensities.

In order to obtain more accuracy in rotational energies for excited vibrational state $v_t = 2$ it is necessary to set up the rotational Hamiltonian as a matrix (H) in eigenvalue equation, $H\psi = E\psi$, and diagonalise to obtain the energy [20-22]. The diagonal matrix elements are given by equation (7). This Hamiltonian can set up for a symmetric top molecule such as CF₃CCH, CF₃CCD, CF₃CN, and OPF₃ [10, 20-30]. It has three different vibrational blocks related to $\ell = 2, 0$ and -2 Figure 6. The vibrational anharmonicity $x_{\ell\ell}\ell^2$ separates the $\ell = \pm 2$ and $\ell = 0$ blocks and they are coupled by the matrix elements q_t^+ and r_t .

In order to explain the form of the spectra we need to consider the energy levels in $v_t = 2$ as given by the Hamiltonian matrix. The diagonal elements are:

$$\begin{aligned} \langle v, \ell, J, k | H/h | v, \ell, J, k \rangle = & v_0 + x_{\ell\ell}\ell^2 + B[J(J+1) - k^2] + Ak^2 - 2A\zeta k\ell \\ & - D_J J^2(J+1)^2 - D_{JK} J(J+1)k^2 - D_K k^4 + \eta_J J(J+1)k\ell + H_J J^3(J+1)^3 + H_{JK} J^2(J+1)k^2 \\ & + H_{KJ}(J+1)k^4 + H_K k^6 + \eta_{JJ} J^2(J+1)^2 k\ell + \eta_K k^3 \eta_\ell + \dots \end{aligned} \tag{7}$$

Where v_0 = pure vibrational frequency which is independent of J, k, ℓ and $x_{\ell\ell}$ is the anharmonicity factor in ℓ . The main off-diagonal elements are the ℓ -doubling elements equation (6).

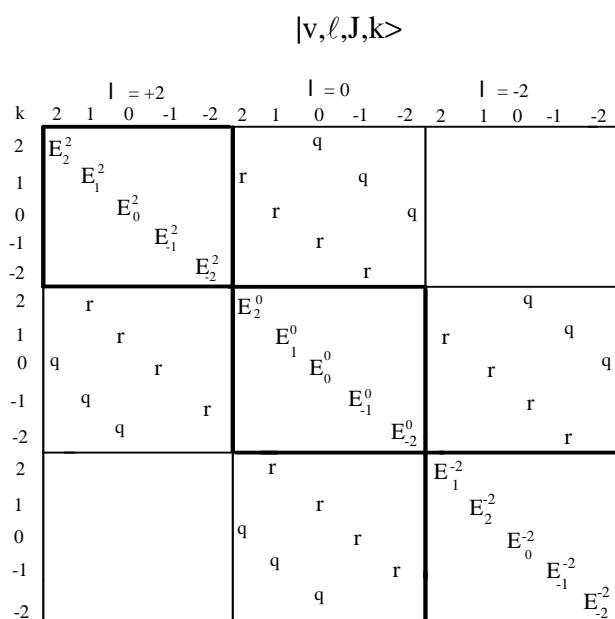


Figure 6. The Hamiltonian matrix for $v_{10} = 2$ state, $J = 2$.

4. Plot of Beff

Plotting of $\frac{v}{2(J+1)}$ against $(J + 1)^2$ can help us to analysis of signals in excited states. Which is described below?

From the theoretical point the frequency expression for transition $J \rightarrow J + 1$ may be put in following effective form:

$$v = (J + 1) A(J,k, \ell) + (J + 1)^3 B(J,k, \ell) \tag{8}$$

where $A(J, k, \ell)$ and $B(J, k, \ell)$ are complicated functions of J, k and ℓ .

Therefore:

$$\frac{v}{(J+1)} = A(J, k, \ell) + (J + 1)^2 B(J, k, \ell) \tag{9}$$

For analysis and investigation of signals, equation (7) can be changed after some abbreviation and alteration to the following form:

$$v = 2B(J + 1) - 4D_J(J + 1)^3 - 2D_{Jk}(J + 1)k^2 \tag{10}$$

$$\pm (q_t^+)(J + 1) \quad \text{for } k\ell - 1 = 0$$

$$\text{or } - \frac{(q_t^+)^2 (J+1)^3}{4(B-A+A\zeta)(k\ell-1)} \quad \text{for } |k\ell-1| \neq 0$$

If both sides of Eq (13) are divided by $2(J+1)$, then:

$$\frac{\nu}{2(J+1)} = B - D_{Jk}k^2 \pm \frac{1}{2}q_t^+ - 2D_J(J+1)^2 \quad \text{for } k\ell-1=0 \quad (11)$$

and

$$\frac{\nu}{2(J+1)} = B - D_{Jk}k^2 - 2D_J(J+1)^2 - \frac{(q_t^+)^2 (J+1)^2}{8(B-A+A\zeta)(k\ell-1)} \quad \text{for } (k\ell-1) \neq 0 \quad (12)$$

Hence plotting $\frac{\nu}{2(J+1)}$ as a function of $(J+1)^2$ will produce a series of lines; two of them relate to

$$k\ell-1=0 \text{ with slope } -2D_J \text{ and intercept } B - D_{Jk}k^2 \pm \frac{1}{2}q_t^+.$$

The $k\ell-1 \neq 0$ states will produce a series of lines with slope

$$-2D_J - \frac{(q_t^+)^2}{8(B-A+A\zeta)(k\ell-1)} \quad (13)$$

and intercept $B - D_{Jk}k^2$. Some of them are nearly parallel to each other and some of them show curvature due to strong ℓ resonance. Equation (10) can be further simplified by taking the term in D_J to the right hand side. This is then an effective B value for the given transition: hence termed BPLOT. Any slope or curvature is then due to the effect of ℓ -resonance.

$$\nu = 2B_{\text{eff}}(J+1) - 4D_J(J+1)^3 \quad (14)$$

$$\therefore B_{\text{eff}} = \frac{\nu}{2(J+1)} + 2D_J(J+1)^2 \quad (15)$$

Plotting of B_{eff} as a function of $(J+1)^2$ will produce a series of lines, each of which belongs to a different $(k\ell-1)$ value. Correlation of observed lines in different J can then be used to help with the assignment.

In $\nu_t = 2$ state the Hamiltonian blocks off into factors which for a C_{3v} molecule are of symmetry species A_1 , A_2 and E . k and ℓ are no longer good quantum numbers but $(k-\ell) \times s$ remains a good symmetry label. In this label s is sign of ℓ , $s = +1$ for $\ell \geq 0$ and $s = -1$ for $\ell < 0$. The spectra are labeled by $(k-\ell)^\ell$ such as 0^{-2} , -1^{-2} and 0^2 in the spectrum of $J=19$ Figure 7.

Accidental resonances can occur when the $\ell = 0$ series are coupled via the q_t^+ term with $\ell = 2$ series. This resonance will affect the frequencies of the $|J, k, \ell\rangle \rightarrow |J+1, k, \ell\rangle$ transitions. The maximum resonance will occur when the energy of state $\ell = 2, k+2$ equals that of $\ell = 0, k$ i.e.

$$E(|J, k, \ell=0\rangle) = E(|J, k+2, \ell=2\rangle) \quad (16)$$

After omitting terms which are the same from both sides of equation (8) this gives:

$$(A - B)k^2 = 4x_{\ell\ell} + (A - B)(k + 2)^2 - 4A\zeta(k + 2) \quad (17)$$

$$\text{Hence } k = \frac{x_{\ell\ell} + (A - B) - 2A\zeta}{A\zeta - (A - B)} \quad (18)$$

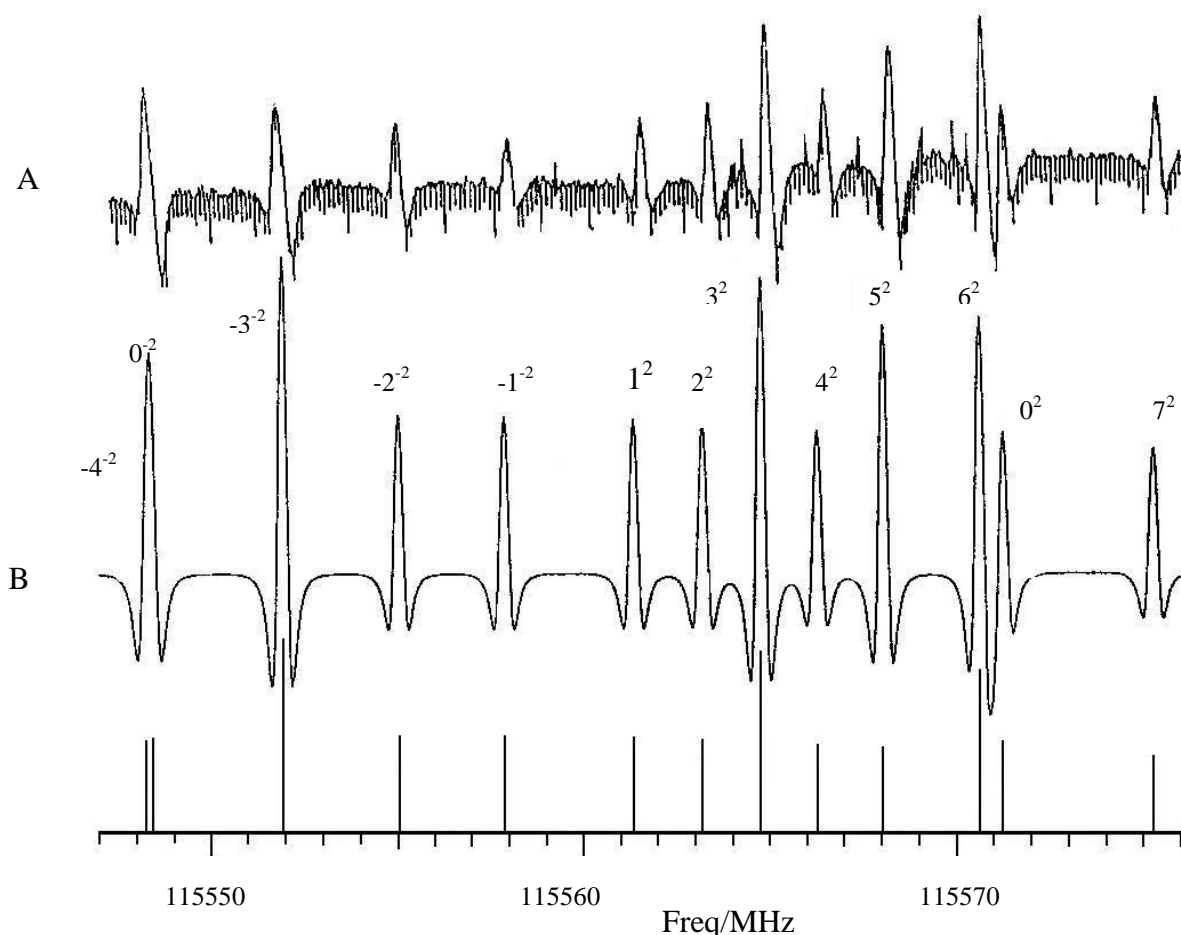


Figure 7. Part of the $J = 19 \rightarrow 20$ spectrum of CF_3CCH in $v_{10} = 2$ state. The top trace (A) is the observed spectrum, the lower (B) is a computer simulation.

If the rotational constants of CF_3CCH from Table 1 are put in equation (18) then k is found to be 9.7. Experimentally the resonance is indeed observed between $k = 9$ and $k = 10$ for this molecule and is independent of J , as expected from equation (18). The calculated spectrum of CF_3CCH in $J = 20 \rightarrow 21$ show this resonance Figure 8. Like this resonance take places in different k values for different molecules which depends on their parameters Table 2.

Figure 9 shows the energy levels as $\ell = 2, 0$ and -2 stacks. The lines between states in adjacent stacks represent the ℓ -type interaction; for example $k = 4$ in $\ell = -2$ is linked to $k = 6, \ell = 0$ and this also interacts with $k = (6 + 2) = 8, \ell = +2$. The interaction results in the energy levels being pushed apart; for example $k = 4$ is shifted up and $k = 6$ is shifted down. The extent of this shift depends on how nearly equal are the energy levels. When they are close, a large shift is obtained. The maximum shift

will occur when the energies are almost equal, see equation (18) and is found in the region of $k \approx 9$. This phenomenon can occur at $k \approx 16$ value for CF_3CCD , Table 2.

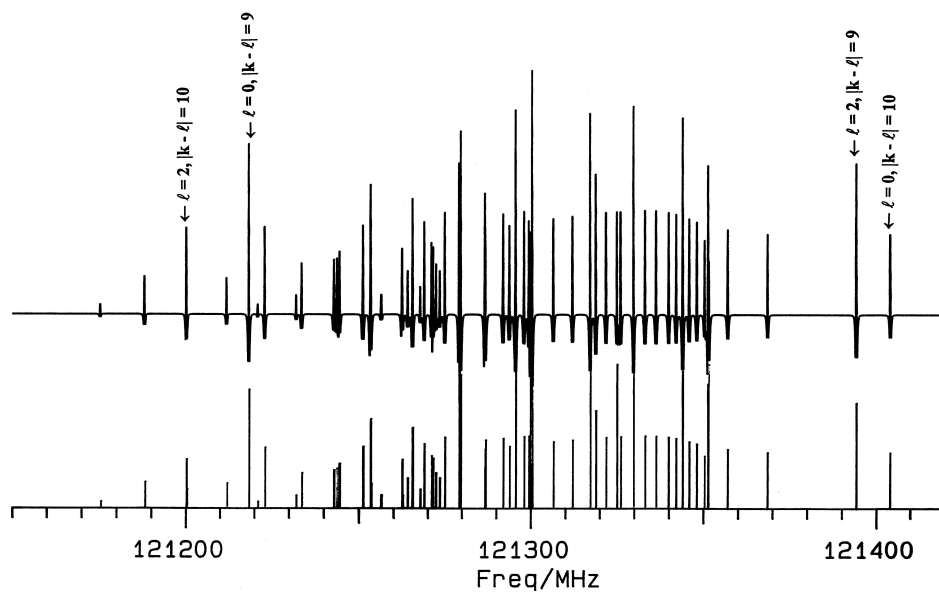


Figure 8. Calculated Spectrum of CF_3CCH in $\nu_{10} = 2$ State. $J = 20 \rightarrow 21$.

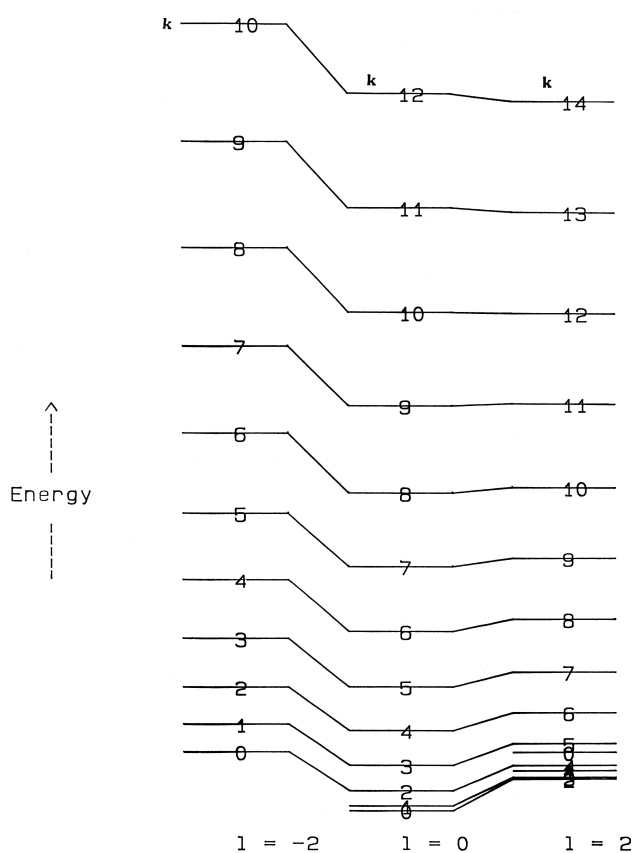


Figure 9. Diagram of energy levels for CF_3CCH in $\nu_{10} = 2$ State.

Table 1. Comparison of the Parameters for the Excited States
 $v_{10} = n$ ($n = 0, 1, 2, 3, 4$) of CF_3CCH .

Parameter	$v_{10} = 0$ [2]	$v_{10} = 1$ [2]	$v_{10} = 2$ [20]	$v_{10} = 3$ [22]	$v_{10} = 4$ [22]
A/MHz	5718.8436*	5718.8436*	5718.8436*	5718.8436*	5718.8436*
B/MHz	2877.9535(78)	2883.4613(1)	2888.9678(3)	2894.3884(75)	2899.7481(14)
A ζ /MHz	-	3293.5541(71)	3293.064(9)	3289.833(162)	3285.999(334)
q $_t^+$ /MHz	-	3.6206334(72)	3.6206334*	3.6154(4)	3.6169(8)
r $_t^+$ /MHz	-	0.0*	0.203(24)	0.165(12)	0.197(9)
D $_J$ /kHz	0.2684784(190)	0.275890(33)	0.2817(2)	0.2888(8)	0.2954(16)
D $_{JK}$ /kHz	6.27696(20)	6.239328(46)	6.2073(15)	6.1628(8)	6.1351(17)
D $_k$ /kHz	-5.23*	-5.23*	-5.23*	-5.23*	-5.23*
η_J /kHz	-	25.50129(89)	25.025(13)	24.977(6)	24.847(8)
η_k /kHz	-	-19.1916(42)	-19.1916*	-15.38(71)	-28.86(177)
D $^{\ell}_J$ /Hz	-	-	-0.3950(62)	-0.395*	-0.395*
D $^{\ell}_{JK}$ /Hz	-	-	-0.967(280)	-0.967*	-0.967*
H $_J$ /mHz	0.03195(110)	0.0348(33)	0.0*	0.0*	0.0*
H $_{JK}$ /mHz	18.0092(170)	-17.824(43)	15.15(96)	15.15*	15.15*
H $_{kJ}$ /mHz	-11.5756(170)	-12.19(66)	0.0*	0.0*	0.0*
H $_k$ /mHz	-	0.0*	0.0*	0.0*	0.0*
q $_J$ /Hz	-	4.29834(36)	0.0*	0.0*	0.0*
$\gamma_{\ell\ell}$ /kHz	-	-	-27.189(86)	-27.030(36)	-28.193(32)
x $_{\ell\ell}$ /MHz	-	-	8260.443(85)	8135.83(2.1)	8056.1(3.1)
η_{JJ} /Hz	-	0.0*	-72.2(67)	-72.2*	-72.2*
f $_{24}$ /kHz	-	-	0.0*	0.0*	-1.039(23)

* Constrained at this value.

Table 2. Resonance phenomena and k value for some different symmetric top molecules.

compound	CF ₃ CCH [20]	CF ₃ CCD [10]	CF ₃ CN [23]	CH ₃ CN [29]	CD ₃ CN[29]
Resonance take place at	k = 9 → 10	k = 16 → 17	k = 21 → 22	k = 3 → 4	k = 3 → 4

The Hamiltonian for $v_{10} = 3$ has four vibrational blocks correspond to the $\ell = +3, +1, -1, -3$ Figure 10. The $\ell = \pm 3$ and $\ell = \pm 1$ blocks are separated in vibrational energy by the anharmonic term . There are, however, couplings between +3 and +1, +1, -1 and -1 and -3, due to the off-diagonal matrix elements q_t^+ and r_t (abbreviated as q and r, respectively, in Figures. 6, 10). The labelling of the eigenvalues of this Hamiltonian by $(k-\ell)s$ where s is 1 for $\ell = +3$ and +1, and -1 for $\ell = -3$ and -1; the symmetry of a given transition can then be easily deduced from the fact that

$$A_1A_2 \text{ symmetry } (k - \ell)s = 3n, \quad n = 0, 1, 2, \dots$$

$$E \text{ symmetry } (k - \ell)s \neq 3n, \quad n = 0, 1, 2, \dots$$

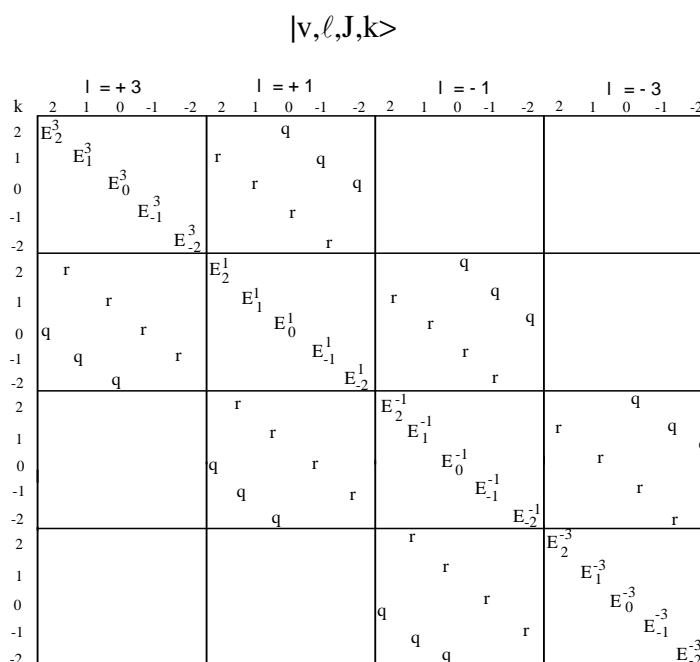


Figure 10. The Hamiltonian matrix for $v_{10} = 3, J = 2$.

The extension to the $v_{10} = 4$ is straightforward. The possible values are + 4,+ 2, 0, - 2, and - 4, so that Hamiltonian consists of five blocks and five series are apparent in the spectra. It is worth noting that, to the order of magnitude that was included in the Hamiltonian.

For $v_{10} = 2$, there are no new parameters in either of the above extension of this Hamiltonian to the cases of $v_{10} = 3$ and $v_{10} = 4$.

5. Results and Discussion

For the CF₃CCH some of the lines belonging to the $\ell = 0$, $\ell = 2$ and $\ell = - 2$ are shown separately in different plots, (Figures 11, 12, 13).

1. In the $\ell = - 2$ series, the lines are nearly parallel to each other, and the distances between these lines become less as $|k - \ell|^*$ s becomes smaller.

2. The two lines 0^{-2} and 0^2 , which are expected to have the same frequency but observed to be are separated, the line 0^{-2} is parallel with $(J + 1)^2$ axis whereas 0^2 line is not Figure 14.

3. The $\ell = 0$ series are located between line 9^0 to line 10^0 but most of them are on the lower frequency side of the spectrum Figure 11.

4. The lines 1^2 to 9^2 are above the 0^{-2} line whereas the other observed lines related to 10^2 and greater are hidden under the 0^{-2} lines Figures. 11,13.

5. Line 10^0 is above line 0^{-2} and lines $11^0, 12^0, 13^0, 14^0$ cross line 0^{-2} but other observed lines belong to the $\ell = 0$ are under the 0^{-2} line Figures. 11,13.

Comparing of Fortrat diagrams of $v_{10} = 3$ and $v_{10} = 4$ with corresponding for $v_{10} = 1$ Figure. 4 and $v_{10} = 3$ [22] is instructive. The $\ell \pm$ series of $v_{10} = 3$ are qualitatively similar to those of $v_{10} = 1$, with ℓ -doublets and strong ℓ -resonance. In the same way the $\ell = 0$ and $+2$ series of $v_{10} = 4$ show a similar resonance to the corresponding series in $v_{10} = 2$ while the $\ell = - 2$ series is relatively unperturbed.

In the case of $v_{10} = 2$ [20], as k increase, the $\ell = 0$ energies come into accidental resonance with those of the positive $(k - \ell)$ s series. These two series of energies are coupled via the q_t^+ . ℓ -resonance matrix element, giving an avoided crossing. Such a resonance is also present for $v_{10} = 3$, but in this case, because the vibrational separation due to the $x_{\ell\ell}$ term is so much larger, this resonance only starts to become obvious at high k [22]. The maximum resonance can occur when

$$E|J, k + 2, \ell = 3\rangle = E|J, k, \ell = 1\rangle \tag{19}$$

Omitting all centrifugal distortion and higher terms and terms which are the same for both states this gives: equation (20).

$$k = \frac{x_{\ell\ell} + (A - B) - 2A\zeta}{A\zeta - (A - B)} \tag{20}$$

If appropriate values input in equation 20 then solving this equation yields a value of k between 19 and 20. There is a slight kink in this diagram which is caused by the accidental degeneracy of the $|J, k, \ell = -1\rangle$ and $|J, k + 4, \ell = +3\rangle$ states which are not directly connected by a matrix element but are coupled in second order by the interaction of both of them with $|J, k = +2, \ell = +1\rangle$. Applying the equation 21 yields a value for the $k = 8.4$ which is indeed where the perturbation is observed.

$$k = \frac{x_{\ell\ell} + 2(A - B) - 3A\zeta}{A\zeta + (A - B)} \tag{21}$$

The $\ell = 0$ and $\ell = \pm 2$ series have separation in $\nu_{10} = 4$ which are close found in the $\nu_{10} = 2$ vibrational state. Consequently, this resonance arises in the same position found for $\nu_{10} = 2$, namely between $k = 9$ and 10 . The $\ell = \pm 4$ series are further away in the energy due to the $x_{\ell\ell} \ell^2$ term. In the $\nu_{10} = 4$ spectrum Figure.15, the transition with $(k - \ell) s = -3$ for the -2 series is split by about 3 MHz in the $J = 20$ spectrum. This splitting is not reproduced by the parameters obtained by extrapolation of the $\nu_{10} = 2$ and $\nu_{10} = 3$ values. In order to account for this, it is necessary to introduce the element $\langle J, k, \ell | f_{24} | J, k+2, \ell-4 \rangle$. This provides a first-order coupling between the otherwise degenerate energies of the $k = +1, \ell = -2$, and $k = -1, \ell = +2$ states which comprise the -3 pair of levels and leads to a splitting of this transition.

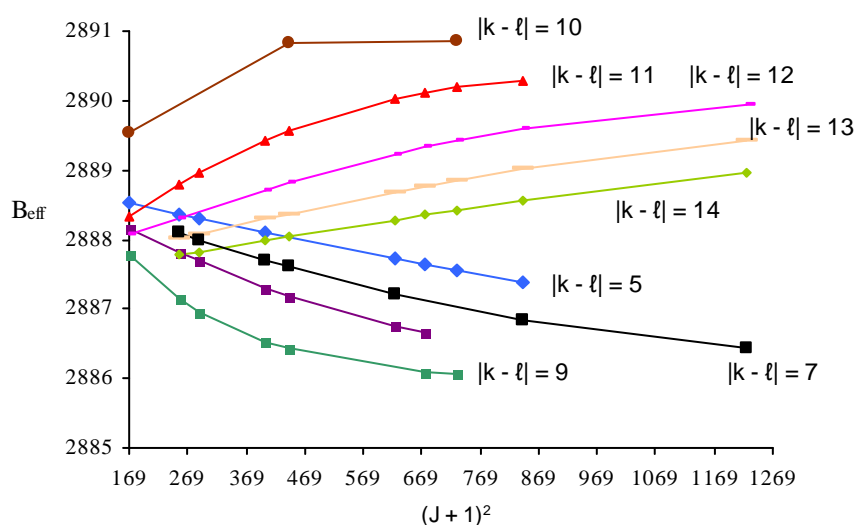


Figure 11. Plot of B_{eff} against $(J + 1)^2$ for $\nu_{10} = 2, \ell = +0$ of CF_3CCH .

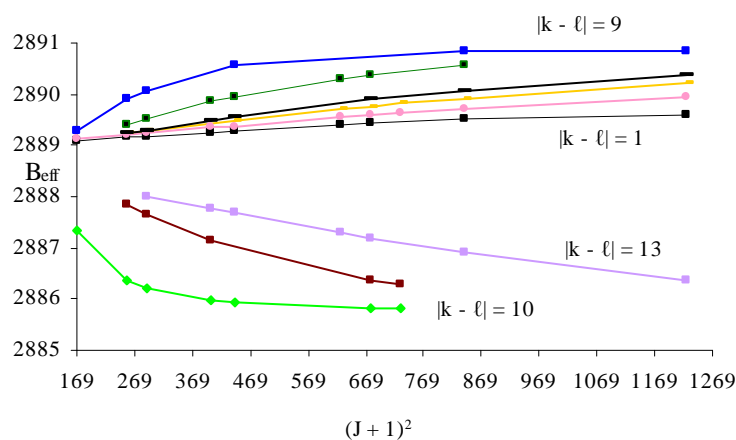


Figure 12. Plot of B_{eff} against $(J + 1)^2$ for $\nu_{10} = 2, \ell = 2$ of CF_3CCH .

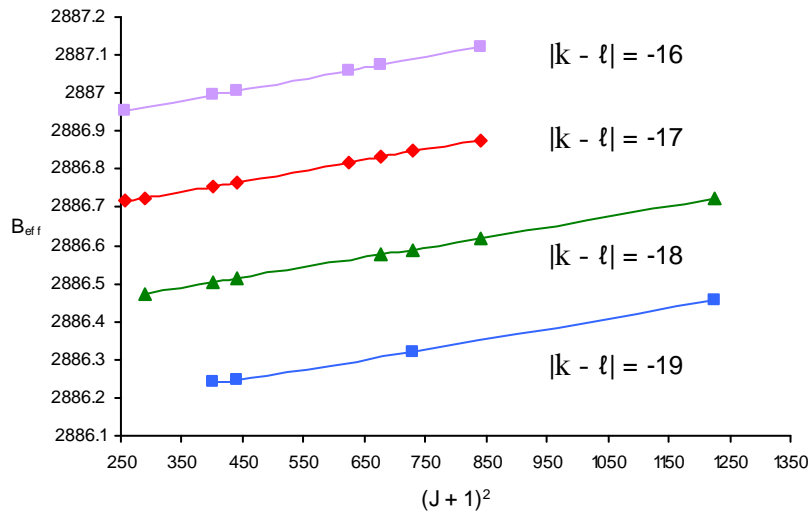


Figure 13. Blot of B_{eff} against $(J + 1)^2$ for $v_{10} = 2$, $l = -2$ of CF_3CCH .

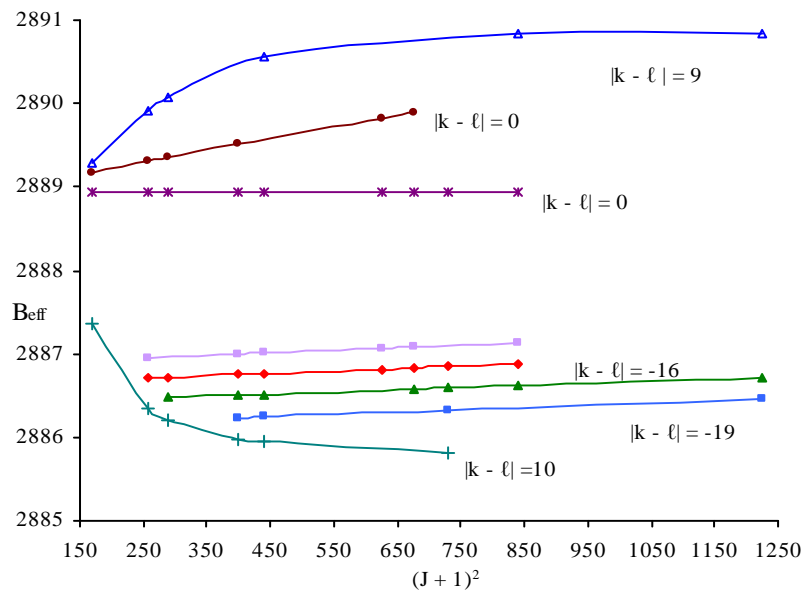


Figure 14. Plot of B_{eff} against $(J + 1)^2$ for selected values of $(k-l)$ s of CF_3CCH .

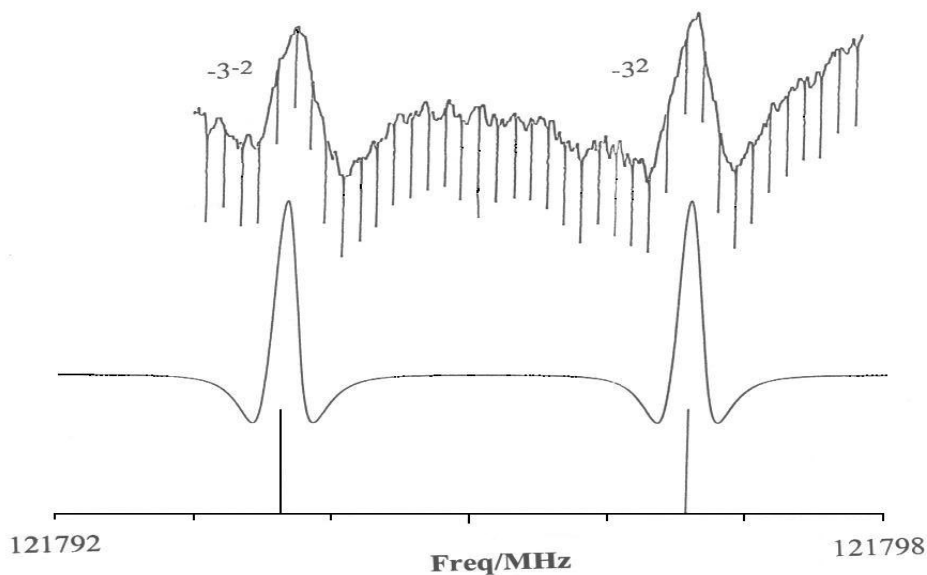


Figure 15. The splitting $(k - \ell)s = -3$ for -2 series state in part of the $J = 20 \rightarrow 21$ spectrum of CF_3CCH in the $\nu_{10} = 4$. The top trace is the observed spectrum, the lower is a computer simulation.

References

- Berney, C.V.; Cousins, L.R.; Miller, F.A. Vibrational Spectra of CF_3CCH , CF_3CCD , and CF_3CCCF_3 . *Spectrochim. Acta* **1963**, *A 19*, 2019-2032.
- Harder, H.; Gerke, C.; Mäder, H.; Cosléou, J.; Bocquet, R.; Demaison, J.D.; Papoušek, K.; Sarka, K. Microwave, Millimeter-Wave, and Submillimeter-Wave Spectra of 1,1,1-Trifluoropropyne: Analysis of the Ground and $\nu_{10} = 1$ Vibrational States and Observation of Direct ℓ - Type Resonance Transitions. *J. Mol. Spectrosc.* **1994**, *167*, 24 – 41.
- Hirota, E.; The ℓ -type doubling transition of PF_3 in the $\nu_4 = 1$ state. *J. Mol. Spectrosc.* **1971**, *37*, 20-32.
- Kawashima, Y.; Cox, A.P. Microwave spectra of CF_3H and CF_3D in the $\nu_6 = 1$ state: Direct ℓ -type resonance transition and $J = 3 \leftarrow 2$. *J. Mol. Spectrosc.* **1976**, *61*, 435-458.
- Harder, H.; Dreizler, H. Proceedings. 12th Colloquium on High Resolution Molecular Spectroscopy, Dijon, France, Poster F36, **1991**.
- Gerke, C.; Harder, H.; Dreizler, H.; Ozier, I.; Moazzen-Ahamadi, A. Proceedings, 12th Colloquium on High Resolution Molecular Spectroscopy, Riccione, Poster O27, **1993**.
- Anderson, W.E.; Trambarulo, R.; Sheridan, J.; Gordy, W. The Microwave Spectrum and Molecular Constants of Trifluoromethyl Acetylene. *Phys. Rev.* **1951**, *82*, 58-60.
- Shoolery, J.N.; Shulman, R.G.; Sheehan, W.F.; Shomaker, V.; Yost, D.M. The Structure of Trifluoromethyl Acetylene from the Microwave Spectrum and Electron Diffraction Pattern. *J. Chem. Phys.* **1951**, *19*, 1364-1369.

9. Mills, I.M. Microwave spectrum of CF₃CCH. *J. Mol. Phys.* **1969**, *16*, 4, 345-348.
10. Motamedi, M.; Carpenter, J.H.; Smith, J. G. The millimetre-wave rotational spectrum of CF₃CCD in the excited vibrational state $\nu_{10} = 2$. *J. Mol. Spectrosc.* **2003**, *221*, 23-30.
11. Motamedi, M.; Haseli, A. Millimeter-Wave Rotational Spectrum of CF₃CCD in the Ground and Excited Vibrational States $\nu_{10} = 1$, *Bull. Chem. Soc. Jpn.* **2006**, *79*,12, 1876-1880.
12. Carpenter, J.H.; Seo, P.Ja.; Whiffen, D.H. The Rotational Spectrum of Chloroform in its Ground and Excited Vibrational States. *J. Mol. Spectros.* **1995**, *170*, 215-227.
13. Cazzoli, G.; Cotti G.; Dore, L.; Kisiel, Z. The Rotational Spectrum of Tertiary Butyl Isocyanide up to 730 GHz – The Observation and Classification of the h₃ splitting. *J. Mol. Spectros.* **1993**, *162*, 467-473.
14. Nielsen, H.H. ℓ -Type Doubling in Polyatomic Molecules and Its Application to the Microwave Spectrum of Methyl Cyanide and Methyl Iso-Cynide. *Phys. Rev.* **1950**, *77*, 130 -135.
15. Grenier-Besson, L.; Amat, G. Rotation Spectrum of Molecules with C_{3v} Symmetry in an Excited Vibrational State $\nu_t = 1$. *J. Mol. Spectrosc.* **1962**, *8*, 22-29.
16. Tarrago, G. Rotational Spectrum of Molecules with C_{3v} Symmetry in an Excited State $\nu_t = 2$. *J. Mol. Spectrosc.* **1970**, *34* , 23-32.
17. Whittle, M.J.; Baker J.G.; Corbelli, G. The Microwave Spectrum of Trifluoroacetonitrile in Excited Vibrational States. *J. Mol. Spectrosc.*, **1971**, *40*, 388-396.
18. Friedrich, A.; Greke, C.; Harder, H.; Mäder, H.; Cosléau, J.; Wlodarczak, G.; Demaison J. Rotational spectrum of CF₃CN in the centimetre, millimetre and submillimetre wave ranges, Observation of direct ℓ -type resonance transitions. *Mol. Phys.* **1997**, *91*, 697-714.
19. Careless, A.J.; Kroto, H.W. Rotational transitions in degenerate vibrational states of C_{3v} symmetric top molecules, with application to CH₃C¹⁵N. *J. Mol. Spectrosc.* **1975**, *57*, 189 – 197.
20. Carpenter, J.H.; Motamedi, M.; Smith, J.G. The Millimeter-Wave Rotational Spectrum of CF₃CCH in the Excited Vibrational State $\nu_{10} = 2$. *J. Mol. Spectrosc.* **1995**, *171*, 468-480.
21. Wötzel, U.; Mäder, H.; Harder, H.; Pracna P.; Sarka, K. The direct ℓ -type resonance spectrum of CF₃CCH in the vibrational state $\nu_{10} = 2$. *Chemical Physics.* **2005**, *312*, 159-167.
22. Carpenter, J.H.; Motamedi, M.; Smith, J.G. The Millimeter-Wave Rotational Spectrum of CF₃CCH in the Excited Vibrational States $\nu_{10} = 3$ and $\nu_{10} = 4$. *J. Mol. Spectrosc.* **1995**, *174*,106-115.
23. Motamedi, M.; Haseli, A. The millimetre-wave rotational spectrum of CF₃CN in the excited vibrational state $\nu_8 = 2$. *J. Mol. Spectrosc.* **2006**, *236*, 91-96.
24. Seo, P.Ja.; Carpenter, J.H.; Smith, J.G. The Millimeter Spectrum of CF₃CN in the Excited Vibrational States $\nu_8 = 3$ and $\nu_8 = 4$. *J. Mol. Spectrosc.* **1997**, *184*, 362-370.
25. Smith, J.G. Millimeterwave spectra of OPF₃ in the vibrationall excited state $\nu_6 = 2$. *J. Mol. Spectrosc.* **1981**, *88*, 126-132.
26. Smith, J.G. Microwave spectrum of phosphoryl trifluoride in vibrationally excited states. *Mol. Phys.* **1976**, *32*, 621-645.
27. Bauer, A.; Maes, S. Effects of an Accidentally Strong Resonance in the Rotational Spectrum of CH₃C¹⁴N and CH₃C¹⁵N in the 2 ν_8 State. *J. Mol. Spectrosc.* **1971**, *40*, 207-216
28. Bauer, A. Rotational Spectrum of Acetonitrile CH₃C¹⁴N and CH₃C¹⁵N in a Doubly Excited Degenerate Vibrational State. *J. Mol. Spectrosc.* **1971**, *40*, 183-206.

29. Chen, W.; Bocquet, R.; Boucher, D.; Demaison, J.; Wlodarczak, G. The Submillimeterwave Rotational Spectra of CH₃CN and CD₃CN. Analysis of the $\nu_8 = 1$ and $\nu_8 = 2$ Excited Vibrational States. *J. Mol. Spectrosc.* **1991**, *150*, 470-476.
30. Wötzel, U.; Mäder, H.; Harder, H.; Pracna, P.; Sarka, K. The direct ℓ -type resonance spectrum of CF₃CCH in the vibrational state $\nu_{10} = 3$. *J. Mol. Struct.* **2006**, 780-781, 206-221.

© 2007 by MDPI (<http://www.mdpi.org>). Reproduction is permitted for noncommercial purposes.